Brain Research 1736 (2020) 146778

Contents lists available at ScienceDirect

Brain Research

journal homepage: www.elsevier.com/locate/brainres

Research report

Characterization of tissue and functional deficits in a clinically translational pig model of acute ischemic stroke

Erin E. Kaiser[a,b,c,1], Elizabeth S. Waters[a,b,c,1], Madison M. Fagan[a,c], Kelly M. Scheulin[a,b,c], Simon R. Platt[a,d], Julie H. Jeon[e], Xi Fang[e], Holly A. Kinder[a,b,c], Soo K. Shin[a,c,f], Kylee J. Duberstein[a,c], Hea J. Park[e], Franklin D. West[a,b,c,*]

[a] Regenerative Bioscience Center, University of Georgia, Athens, GA, United States
[b] Neuroscience Program, Biomedical and Health Sciences Institute, University of Georgia, Athens, GA, United States
[c] Department of Animal and Dairy Science, College of Agricultural and Environmental Sciences, University of Georgia, Athens, GA, United States
[d] Department of Small Animal Medicine and Surgery, College of Veterinary Medicine, University of Georgia, Athens, GA, United States
[e] Department of Foods and Nutrition, College of Family and Consumer Sciences, University of Georgia, Athens, GA, United States
[f] Department of Pharmaceutical and Biomedical Sciences, Interdisciplinary Toxicology Institute, University of Georgia, Athens, GA, United States

HIGHLIGHTS

- Acute ischemic stroke impaired the white matter integrity of pig internal capsules.
- Increased hemispheric swelling and hemorrhage resulted in notable midline shift.
- Pig neutrophil-to-lymphocyte levels replicate patient outcomes at acute timepoints.
- Evidence of post-stroke depression was observed via reduced exploratory behavior.
- Pigs replicated patient deficits through gait impairments in the hemiplegic limb.

ARTICLE INFO

Keywords:
Brain ischemia
Gait analysis
Magnetic resonance imaging
Porcine
Acute stroke

ABSTRACT

The acute stroke phase is a critical time frame used to evaluate stroke severity, therapeutic options, and prognosis while also serving as a major tool for the development of diagnostics. To further understand stroke pathophysiology and to enhance the development of treatments, our group developed a translational pig ischemic stroke model. In this study, the evolution of acute ischemic tissue damage, immune responses, and functional deficits were further characterized. Stroke was induced by middle cerebral artery occlusion in Landrace pigs. At 24 h post-stroke, magnetic resonance imaging revealed a decrease in ipsilateral diffusivity, an increase in hemispheric swelling resulting in notable midline shift, and intracerebral hemorrhage. Stroke negatively impacted white matter integrity with decreased fractional anisotropy values in the internal capsule. Like patients, pigs showed a reduction in circulating lymphocytes and a surge in neutrophils and band cells. Functional responses corresponded with structural changes through reductions in open field exploration and impairments in spatiotemporal gait parameters. Characterization of acute ischemic stroke in pigs provided important insights into tissue and functional-level assessments that could be used to identify potential biomarkers and improve preclinical testing of novel therapeutics.

1. Introduction

Every year, approximately 6.2 million patients die from stroke, while 5 million stroke survivors are left permanently disabled (WHO, 2004). Although hundreds of therapeutics have sought to mitigate patient morbidity and mortality, only two Food and Drug Administration (FDA)-approved therapies are currently available to ischemic stroke patients, tissue plasminogen activator (tPA) and endovascular thrombectomy (WHO, 2004). The limitations of these therapies including short administration windows (< 4.5 h) and associated risk

* Corresponding author at: University of Georgia, 425 River Road, Office 316, Athens, GA 30602, United States.
E-mail address: westf@uga.edu (F.D. West).
[1] These authors contributed equally to this work.

https://doi.org/10.1016/j.brainres.2020.146778
Received 10 January 2020; Received in revised form 4 March 2020; Accepted 10 March 2020
Available online 16 March 2020
0006-8993/ © 2020 The Authors. Published by Elsevier B.V. This is an open access article under the CC BY-NC-ND license (http://creativecommons.org/licenses/BY-NC-ND/4.0/).

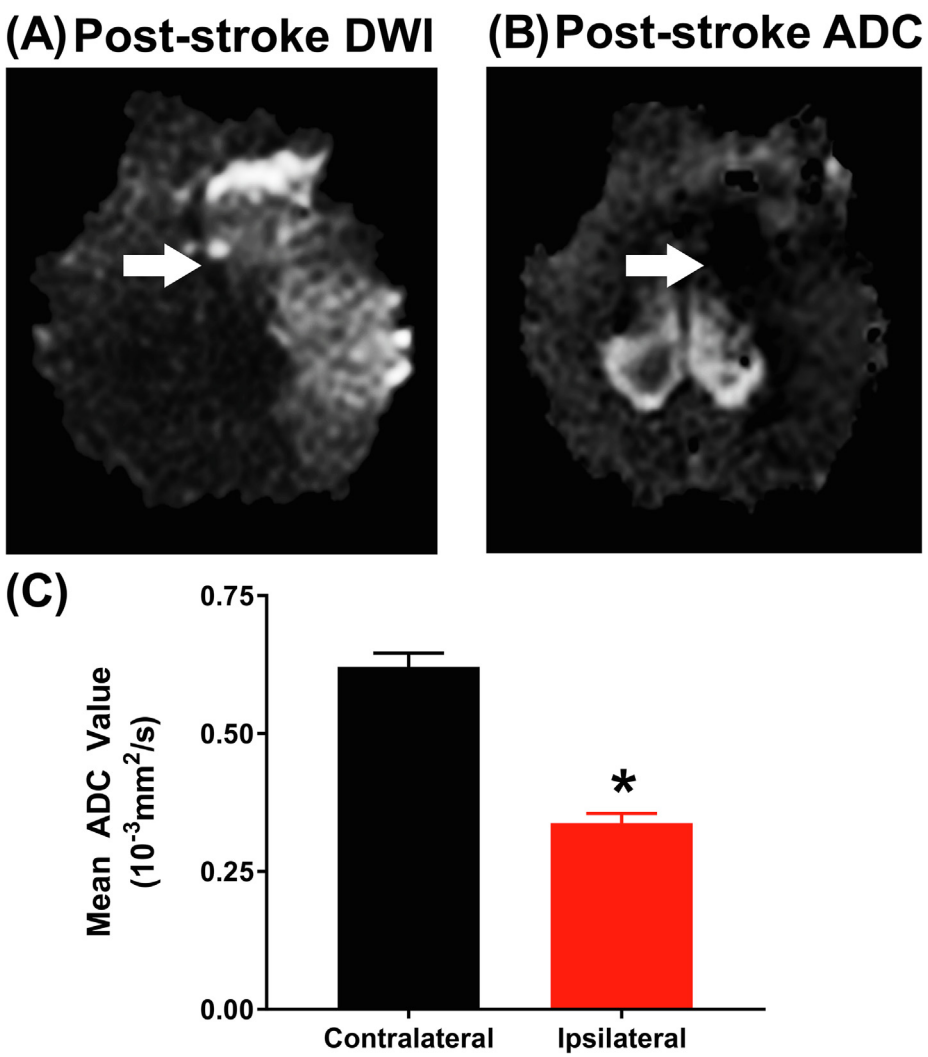

Fig. 1. MCAO induced acute ischemic infarction and decreased diffusivity. DWI sequences exhibited territorial hyperintense lesions of 9.91 ± 1.40 cm^3 characteristic of an edematous injury (A, white arrow). ADC maps revealed signal void indicative of restricted diffusion and cytotoxic edema (B, white arrow). Ipsilateral ROIs exhibited a significantly ($p \leq 0.0001$) lower ADC value relative to the contralateral hemisphere (0.34 ± 0.02 vs. 0.62 ± 0.03 x$10^{-3}$$mm^2$/s, respectively; C). * indicates significant difference between hemispheres.

factors (intracerebral hemorrhage) have promoted the continued investigation of novel stroke therapies. In order to improve preclinical translation, the Stem Cell Emerging Paradigm in Stroke (STEPS) and the Stroke Therapy Academic Industry Roundtable (STAIR) consortiums strongly recommend testing in gyrencephalic, large animal models (Savitz et al., 2011; Fisher et al., 2009). Although the use of non-human primates (NHPs) is an advantageous preclinical model due to the remarkable anatomical similarity between NHPs and humans, the extensive limitations of cost, housing facilities, veterinary care, and ethical challenges associated with NHPs warrant further investigation in alternative large animal species (Kaiser, 2019). Consequently, a pig ischemic stroke model has been developed with brain anatomy and pathophysiology similar to humans (Platt et al., 2014). Follow up studies have utilized this representative animal model to assess the safety and efficacy of putative therapies (neural stem cells and extracellular vesicles) to better predict patient outcomes in clinical trials (Baker et al., 2017; Webb et al., 2018).

Magnetic resonance imaging (MRI) assessment of stroke patients is standard in diagnosing and predicting clinical outcomes (Vilela and Rowley, 2017; Rudkin et al., 2018). Specifically, acute diffusion weighted imaging (DWI) lesion volumes have frequently mirrored final patient lesion volumes and correlated with stroke severity as assessed by Modified Rankin Scale (mRS) and National Institutes of Health Stroke Scale (NIHSS) scores (Tong et al., 1998; Barber et al., 1998; Attye et al., 2012). Pig DWI sequences reliably detected lesion location, age, and size with high sensitivity and specificity, thus highlighting the importance of this translational tool (Warach et al., 1995; Lutsep et al., 1997; Lovblad et al., 1998). Similarities in cerebral white matter (WM) composition between pigs and humans (> 60%) is critically important in modeling ischemia as white and gray matter exhibit differing metabolisms and sensitivities to hypoxia (Baltan et al., 2008; Nakamura et al., 2009). Disruptions in WM integrity and progressive remodeling of contralateral WM tracts have been associated with poor motor function in patients and was similarly observed in pigs' with notable deteriorations in internal capsule (IC) integrity and gait performance post-stroke (Liu et al., 2015; Wang et al., 2016).

Gait analysis is frequently employed in clinical settings to measure functional deficits as quantitative assessments in motor pathologies may serve to predict long-term recovery and efficacy of treatments in patients (Li et al., 2019;19(7).; Boudarham et al., 2013). Patients have demonstrated significant alterations in foot placement, stride length, and ambulation speed all of which are powerful indicators of long-term recovery (Nascimento et al., 2015; Hak et al., 2015; Peterson et al., 2010; Nolan et al., 2015; De Nunzio et al., 2014). Pigs provided a unique opportunity to study post-stroke changes due to anatomical similarities in the size of the prefrontal cortex and cerebellum; key motor

function brain regions (Lind et al., 2007). In addition, comparable somatotopical organization of the motor and somatosensory cortices between pigs and human is critically important in modeling acute ischemic stroke motor impairments (Craner and Ray, 1991). Understanding motor impairments is essential in planning rehabilitation efforts in order to restore ambulatory independence (Michael et al., 2005).

The objective of this study was to utilize clinically relevant assessment modalities to characterize acute (< 48 h) ischemic stroke using a pig middle cerebral artery occlusion (MCAO) model. Researchers believed this would provide a translational platform to study potential diagnostic modalities and therapeutic interventions. This study provides novel characterization of acute intracerebral hemorrhage (ICH), IC deterioration, white blood cell changes, quantifiable deficits in exploratory perimeter sniffing and gait performance, thus providing compelling evidence that pigs could serve as a valuable tool to further characterize acute ischemic stroke pathologies.

2. Results

2.1. MCAO induced acute ischemic infarction and decreased diffusivity

To confirm ischemic stroke 24 h post-MCAO, MRI DWI (Fig. 1A) and T2 Fluid Attenuated Inversion Recovery (T2FLAIR) sequences were assessed. DWI and T2FLAIR sequences exhibited territorial hyperintense lesions, while hypointense lesions on corresponding Apparent Diffusion Coefficient (ADC) maps (Fig. 1B) confirmed areas of restricted diffusion indicative of cytotoxic edema, thus confirming permanent cauterization of the middle cerebral artery (MCA) resulted in ischemic stroke. DWI sequences revealed an average lesion volume of 9.31 ± 1.29 cm^3 (Fig. 1A). ADC sequences revealed significantly ($p < 0.001$) decreased diffusivity within ischemic lesions when compared to identical regions of interest in the contralateral hemisphere (0.34 ± 0.02 vs. 0.62 ± 0.03 × $10^{-3}mm^2/s$, respectively; Fig. 1B–C).

2.2. Ischemic stroke resulted in acute hemispheric swelling, hemorrhage, and loss of WM integrity

Analysis of T2Weighted (T2W) sequences at 24 h post-stroke revealed a significant ($p < 0.01$) increase in ipsilateral hemisphere volume indicative of cerebral swelling when compared to the contralateral hemisphere (25.99 ± 1.78 vs. 22.49 ± 1.40 cm^3, respectively; Fig. 2A–C) and an associated midline shift (MLS) of 2.48 ± 0.55 mm (Fig. 2A–B; red lines). Acute ICH was observed via T2Star (T2*) sequences with a consistent mean hemorrhage volume of 1.73 ± 0.07 cm^3 (Fig. 2D–E, white arrow), which suggested portions of the ischemic infarct may have undergone hemorrhagic transformation (HT). Interestingly, ICH in the basal ganglia and surrounding structures was associated with limb weakness (Supplemental Fig. 1; white arrows). Gross pathological findings also revealed the presence of ICH in the cerebellum and along the ventral cranial brain stem which coincided with pronounced ataxia. To assess changes in WM integrity, fractional anisotropy (FA) values of the ICs were evaluated 24 h post-stroke and revealed a significant ($p < 0.01$) decrease in the ipsilateral IC when compared to the contralateral side (0.17 ± 0.01 vs. 0.23 ± 0.01 respectively; Fig. 3A-C; white arrow). Collectively, MRI results demonstrated MCAO led to tissue-level damage including ischemic infarction, decreased diffusivity, hemispheric swelling, pronounced MLS, ICH, and disrupted WM integrity.

2.3. Ischemic stroke increased circulating neutrophil levels and decreased circulating lymphocyte levels

To determine changes in immune cell response to acute ischemic stroke, band neutrophils (Fig. 4A–B), neutrophils (Fig. 4C–D), and lymphocytes (Fig. 4E–F) were assessed via manual cell counts. Band neutrophils significantly ($p < 0.05$) increased 12 h post-stroke compared to pre-stroke (5.50 ± 1.09% vs. 1.92 ± 0.99% respectively; Fig. 4B). Similarly, the number of circulating neutrophils was significantly ($p < 0.05$) increased at 4- and 12-hours post-stroke when compared to pre-stroke (43.60 ± 5.00% and 48.90 ± 5.01% vs. 26.50 ± 4.57%, respectively; Fig. 4D) with a trending ($p = 0.06$) difference observed at 24 h. Circulating lymphocytes were significantly ($p < 0.05$) decreased at 4, 12, and 24-hours post-stroke compared to pre-stroke (31.57 ± 4.64%, 25.60 ± 4.66%, and 26.54 ± 4.65% vs. 44.83 ± 4.26% respectively; Fig. 4F). These results demonstrated stroke resulted in an increase in circulating band neutrophils and neutrophils and a decrease in circulating lymphocytes which indicated

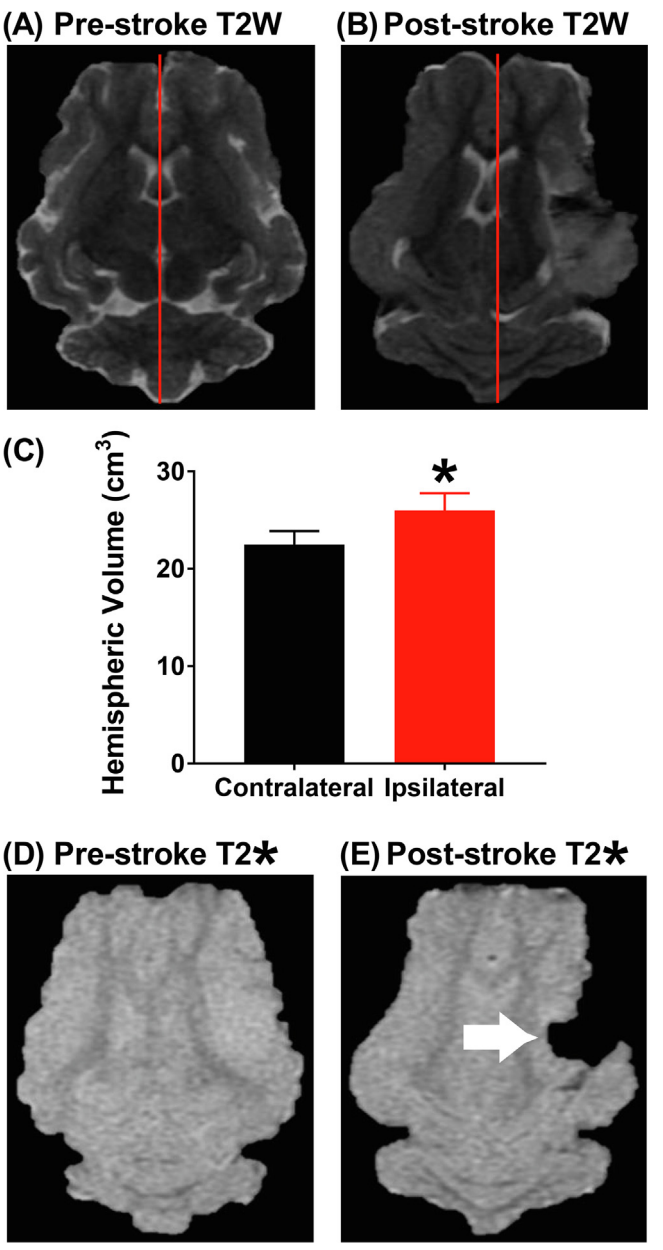

Fig. 2. Ischemic stroke resulted in hemispheric swelling, consequent MLS, and ICH. T2W sequences revealed increased ($p < 0.01$) swelling of the ipsilateral hemisphere (25.99 ± 1.78 vs. 22.49 ± 1.40 cm^3; A-C) resulting in a pronounced MLS of 2.48 ± 0.55 mm compared to pre-stroke imaging (A and B, red lines). Characteristic hypointense ROIs indicated the presence of ipsilateral ICH when compared to pre-stroke T2* sequences (1.73 ± 0.17 cm^3, D and E, white arrow).

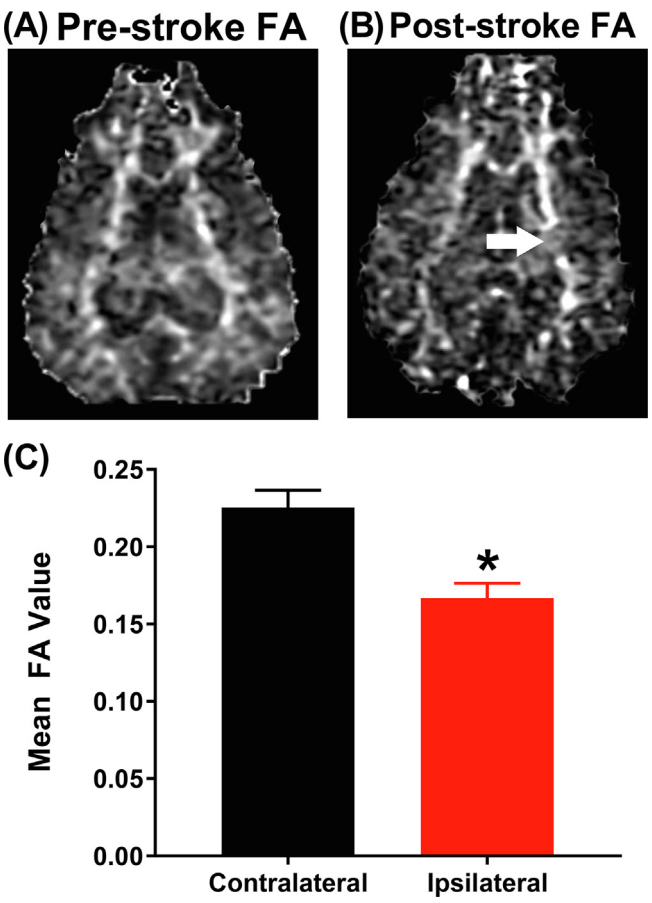

Fig. 3. Ischemic stroke diminished WM integrity of the IC. Pre-stroke the left and right IC possess similar WM integrity (A). 24 h post-stroke, the ipsilateral IC exhibited a disruption in WM integrity (B, white arrow). Further analysis revealed a significant ($p < 0.01$) decrease in the ipsilateral IC FA value when compared to the contralateral IC (0.17 ± 0.01 vs. 0.23 ± 0.01 respectively; C). * indicates significant difference between hemispheres.

an acute post-stroke immune response.

2.4. Ischemic stroke decreased exploratory behavior during open field testing

Changes in perimeter sniffing, a typical exploratory behavior exhibited by pigs, was assessed during open field (OF) testing 48 h post-stroke. Representative Ethovision XT movement tracings revealed a significant decrease ($p < 0.01$) in perimeter sniffing (red lines) between pre- (Fig. 5A) and post-stroke (Fig. 5B) time points (26.00 ± 4.02 vs. 13.00 ± 2.94 times, respectively, Fig. 5C). Although no significant differences were noted for OF velocity or distance traveled, these parameters decreased post-stroke (14.33 ± 1.42 vs. 13.37 ± 3.03 cm/s and 85.48 ± 8.48 vs. 79.74 ± 19.59 m, respectively). These results suggested MCAO impaired normal pig exploratory behaviors.

2.5. Ischemic stroke resulted in spatiotemporal gait deficits

Key spatiotemporal gait parameters were analyzed pre- and 48 h post-stroke to detect potential impairments in motor function. Significant ($p < 0.01$ and 0.001, respectively) decreases were noted in the velocity and cadence at 48 h post-stroke compared to pre-stroke (61.01 ± 8.39 vs. 162.9 ± 12.73 cm/s and 61.01 ± 5.91 vs. 126.44 ± 3.72 steps/min, respectively, Fig. 6A–B). Further changes were noted in measurements of the contralateral left forelimb (LF). The swing percent of cycle significantly ($p < 0.01$) decreased demonstrating pigs spent more time with the LF in contact with the ground at 48 h post-stroke compared to pre-stroke suggesting an increased need for support (30.70 ± 2.12 vs. 48.89 ± 2.35%, respectively, Fig. 6C). A significant ($p < 0.01$) decrease in LF stride length was observed at 48 h post-stroke compared to pre-stroke (59.04 ± 3.85 cm vs. 76.72 ± 4.60 cm, respectively, Fig. 6D). Cycle time of the LF significantly ($p < 0.01$) increased signifying a slower gait at 48 h post-stroke compared to pre-stroke (1.02 ± 0.09 vs. 0.48 ± 0.01 sec, respectively, Fig. 6E). Finally, the mean pressure exhibited by the LF significantly ($p < 0.01$) decreased at 48 h post-stroke compared to pre-stroke (2.62 ± 0.03 vs. 2.82 ± 0.03 arbitrary units (AU), respectively, Fig. 6F). Deficits in the measured gait parameters indicated stroke led to substantial motor impairments at acute time points.

3. Discussion

In this study, we observed and characterized acute stroke injury severity, prognostic biomarkers, and potential therapeutic targets utilizing clinically relevant MRI, immune, behavior, and motor function tests in a translational pig ischemic stroke model. This model resulted in consistent lesion volumes that were comparable to patient DWI lesion volumes with similar impairments in functional performance (Lovblad et al., 1997). Ischemic injury produced cerebral swelling and consequent MLS as well as notable ICH, all of which are strongly associated with stroke patient morbidity (Schellinger et al., 1999; Jokinen et al., 2011). In addition, reductions in IC WM integrity correlated with contralateral deteriorations in motor function parameters commonly assessed in patients (Ahmad et al., 2015; Srikanth et al., 2009). Likewise, MCAO led to an acute immune response marked by an increase in circulating neutrophils and a corresponding decrease in circulating lymphocytes; a key biomarker for identifying ischemic stroke patients at risk for ICH development, and thus influencing the use of tPA (Pikija et al., 2018; Guo et al., 2016; Song et al., 2018). Functional assessments exposed impaired exploratory behavior and motor function performance that affected both spatiotemporal parameters and weight distribution, all of which parallel clinical functional outcomes in stroke patients (Clark et al., 2006; Alexander et al., 2009). By further understanding these physiological hallmarks and exploiting the similarities between pigs and humans, this pig ischemic stroke model could be utilized to decrease the translational gap between preclinical rodent studies and clinical trials.

DWI has proven to be a critical assessment tool frequently utilized in clinical settings for its early diagnostic and prognostic capabilities in acute ischemic stroke patients (Kumar et al., 2010; Saenger and Christenson, 2010). Given that pig brains are approximately 7.5 times smaller than human brains, mean lesion volumes of 9.31 ± 1.29 cm^3 at 24 h post-stroke are similar to acute DWI lesion thresholds of 72 cm^3 in patients with major cerebral artery occlusions (Yoo et al., 2010). Often preclinical stroke models have relied on T1 or T2W MRI sequences which are typically delayed in early recognition of cerebral ischemia and do not account for diffusion abnormalities that may evolve into infarction (Huisman, 2003; Payabvash et al., 2017). DWI lesion measurements overcome this limitation. Common pathological features of human ischemia were also observed in our model including significant restricted diffusion in the parietal, limbic, and temporal lobes (Merino and Warach, 2010; Assemlal et al., 2011). Pigs primarily demonstrated cytotoxic edema at 24 h as indicated by ADC maps which later evolved into vasogenic edema. This holds significant value as cytotoxic edema in patients is considered reversible whereas vasogenic edema is identified as largely irreversible (Jha, 2003). Furthermore, advances in translational research now identify cytotoxic edema as the primary promoter of ionic edema, vasogenic edema, and complete HT (Liang et al., 2007). A pig model that is representative of this human condition could not only improve the understanding of these molecular mechanisms, but could also lead to the development of

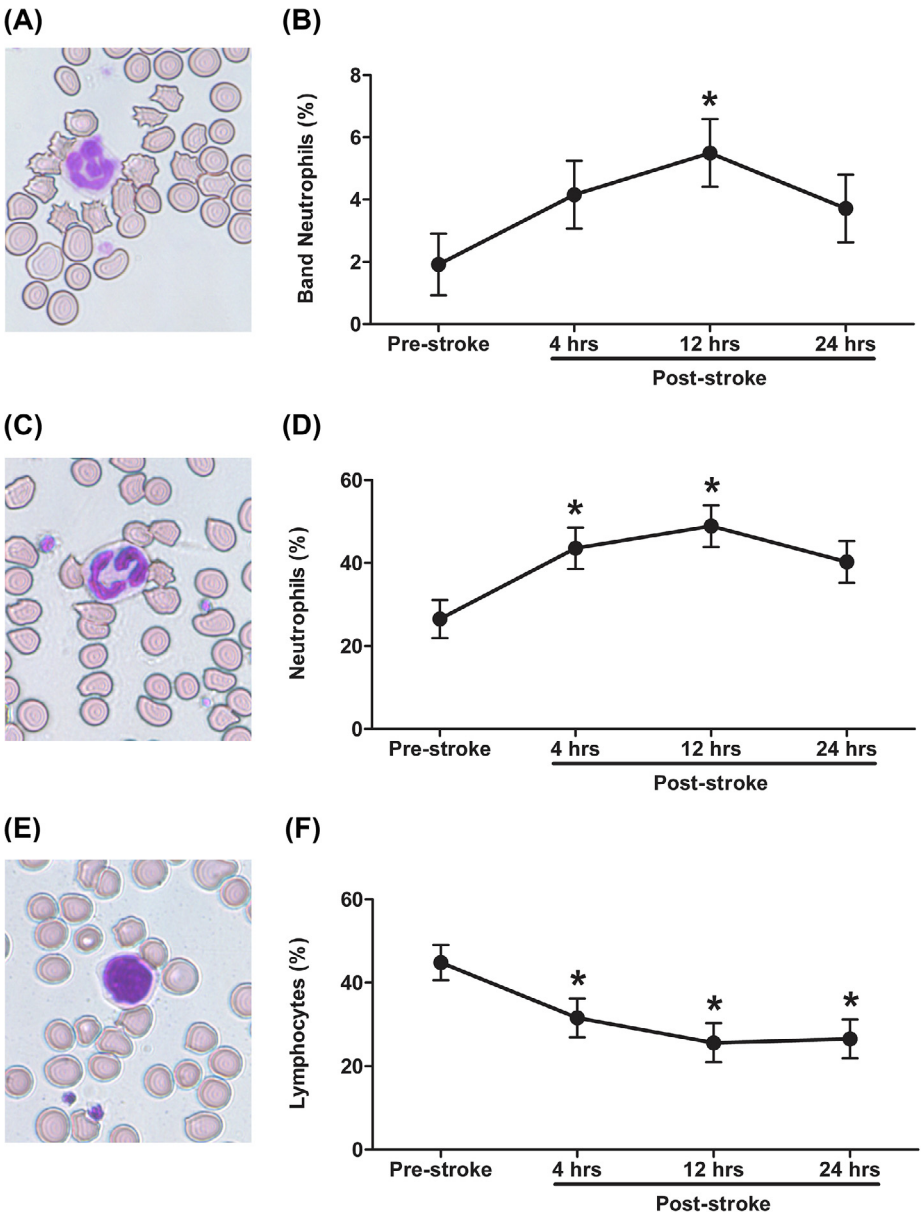

Fig. 4. Ischemic stroke led to increased circulating neutrophil levels and decreased circulating lymphocyte levels. Band neutrophils showed a significant ($p < 0.05$) increase 12 h post-stroke when compared to pre-stroke (5.50 ± 1.09% vs. 1.92 ± 0.99% respectively; A, B). Circulating neutrophils were significantly ($p < 0.05$) increased at 4- and 12-hours post-stroke relative to pre-stroke (43.60 ± 5.00% and 48.90 ± 5.01% vs. 26.50 ± 4.57%, respectively; C, D). Circulating lymphocytes were significantly ($p < 0.05$) decreased at 4, 12, and 24-hours post-stroke compared to pre-stroke (31.57 ± 4.64%, 25.60 ± 4.66%, and 26.54 ± 4.65% vs. 44.83 ± 4.26%; E, F). * indicates significant difference between pre-stroke and post-stroke time points.

pharmacological interventions effective against cerebral edema and the secondary injury cascade produced by this sequela.

Cerebral edema and consequent hemispheric swelling are serious stroke complications that result in rapid neurological deterioration and a disproportionately high 30-day patient mortality rate of 60–80% (Berrouschot et al., 1998; Hacke et al., 1996). Crudely managed via osmotic diuretics and/or decompressive craniectomies, patients are in desperate need for more effective and less invasive pharmacotherapies (Arnaout et al., 2011; Vahedi et al., 2007; Wang et al., 2011). These needs have been met with poor therapeutic translation due to discrepencies in lissencephalic small animal stroke models including limited cerebral edema and swelling as well as variable MLS and mortality rates (O'Collins et al., 2006; Kotwica et al., 1991). Specifically in endothelin-1 (ET-1) rodent stroke models, animals exhibit a dose-dependent ischemic lesion with marginal ischemic edema making this model less suited for studying acute stroke pathophysiology (Schirrmacher et al., 2016; Hughes et al., 2003; Fluri et al., 2015). In contrast, our pig stroke model exhibited increased ipsilateral hemisphere swelling due to the development of cytotoxic edema and consequent MLS within 24 h post-stroke. These observations are in keeping with other large animal models of stroke, in which permanent ovine MCAO demonstrated cerebral edema and MLS (Wells et al., 2015). These physiological responses post-ischemic stroke are frequently associated with different levels of consciousness and serve as a predictive indicator of patient prognosis (Ropper, 1986; Treadwell and Thanvi, 2010). Furthermore, clinical studies indicate quantification of MLS can predict cerebral herniations and subsequent death prior to clinical signs and are a clinically relevant feature of this pig stroke model (Walberer et al., 2007).

Although MRI techniques have become increasingly valuable in characterizing and refining the field's understanding of ICH, the time course and underlying mechanisms remain poorly understood due to variability in the onset, size, and location of ICH in current stroke animal models (Alharbi et al., 2016). Often resulting from HT in ischemic stroke patients, ICH incidence ranges from 38 to 71% in autopsy studies and from 13 to 43% in computed tomography (CT) studies (Jaillard et al., 1999). Furthermore, when ICH occupies > 30% of the infarct zone, it has been correlated with early neurological deterioration and a significant increase in mortality rates 90 days post-ischemic stroke (D'Amelio et al., 2014; Fiorelli et al., 1999). T2* sequences showed consistent mean hemorrhage volumes between pigs, indicating MCAO caused loss of macro- and microvessel integrity. The classical clinical

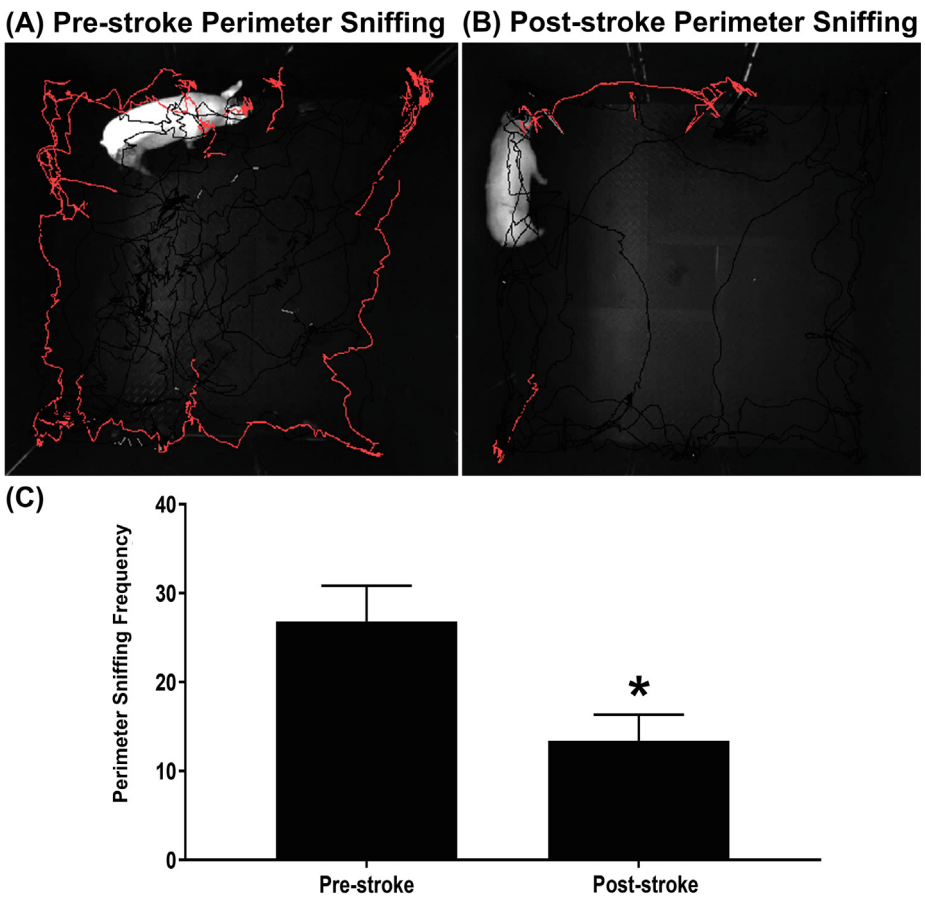

Fig. 5. MCAO led to functional disabilities and behavioral abnormalities. Ethovision XT tracking software was used during OF testing to automatically assess differences in perimeter sniffing (red lines) pre-stroke (A) and post-stroke (B). Exploratory perimeter sniffing frequencies were significantly ($p < 0.05$) reduced at 48 h post-stroke compared to pre-stroke observations (26.00 ± 4.02 vs. 13.00 ± 2.94 times, respectively; C), whereas distance traveled was not ($p = 0.77$; 85.48 ± 8.48 vs. 79.74 ± 19.59 m). Black lines were indicative of non-perimeter sniffing and other non-exploratory behaviors (e.g. ambulation, laying down, escape behavior). * indicates a significant difference from pre-stroke.

presentations of ICH were replicated in our model through the progression of neurological deficits within hours post-stroke including decreased consciousness, head-pressing, vomiting, facial paralysis, and limb weakness (Caceres and Goldstein, 2012; Sahni and Weinberger, 2007). In previous studies, early neurological deterioration was primarily attributed to cerebral edema and lesion volume; however, recent clinical, pathological, MRI, and CT studies suggest hemorrhage into ischemic tissues is a major contributor to poor clinical outcome, making ICH a novel target of preclinical studies (Castro et al., 2017; Zhang et al., 2014; Yaghi et al., 2017). By replicating both tissue-level and neurological presentations unique to ICH, our model presents an exciting new platform for testing hemostatic therapies and surgical interventions.

For the first time, it was observed MCAO led to reduced WM integrity in the IC 24 h post-stroke in the pig model. This subcortical structure is highly involved in communication between the cerebral cortex and brainstem resulting in profound muscle weakness and inhibited perception of sensory information of the patient's face, arm, trunk, and leg post-stroke (Biesbroek et al., 2017). Studies using Functional Ambulatory Categories found patients with IC lesions experience persistent (> 6 months) functional motor deficits; requiring aids for balance and support during ambulation (Lee et al., 2017). As the right IC transmits nerve signals for movement of the left side of the body, our pig MCAO model closely replicated post-stroke deficits as seen through a decrease in spatiotemporal gait parameters of the hemiplegic limb including LF stride length and LF swing percent of cycle. Similarly, stroke patients exhibit decreased stride length and swing phases in the hemiplegic limb (Roth et al., 1997; Titianova and Tarkka, 1995). The mean pressure of pigs' LF limb was also decreased due to overall weakness and reduced use of the hemiplegic limb (Hidler et al., 2007). Stroke pigs compensated for limb weakness and balance impairments by taking shorter, slower steps, thus reducing their velocity and cadence to better stabilize their gait. In a comparable human study utilizing the analogous GAITRite system, WM lesions corresponded with poorer gait outcomes as measured by step length and abnormal cadence (Srikanth et al., 2009). These manifestations complemented our previous publications and provided support for the continued use of quantitative gait analysis for stroke severity and therapeutic recovery evaluations (Webb et al., 2018; Duberstein et al., 2014).

Immune and inflammatory responses have been shown to play a key role in the sequelae of ischemic stroke (Chamorro and Hallenbeck, 2006). Within the first few hours after stroke, neutrophils are recruited to the site of injury and release cytokines, chemokines, free oxygen radicals, and other inflammatory mediators (Kleinig and Vink, 2009). In this study, we observed a significant increase in neutrophils at 4- and 12-hours post-stroke. Neutrophil release of inflammatory mediators has been directly associated with cell damage or death as well as damage to the vasculature and extracellular matrices (Kleinig and Vink, 2009). Neutrophils have been implicated to play a significant role in blood brain barrier disruption and HT following ischemic stroke, which may explain one potential mechanism for HT observed 24 h post-stroke in this study (Guo et al., 2016). Conversely, acute ischemic stroke has been shown to induce a rapid and long-lasting suppression of circulating immune cells such as lymphocytes that can lead to increased susceptibility of systemic infections after stroke (Haeusler et al., 2008). In this study, we observed a significant decrease in lymphocytes at 12 and 24 h post-stroke, consistent with reports that stroke in humans induces immediate loss of lymphocytes that is most pronounced at 12 h post-stroke (Vogelgesang et al., 2008). Though the exact mechanisms by which lymphocytes mediate immunosuppression post-stroke remain unclear, clinical evidence supports that lower levels of lymphocytes are a sign of poor long-term functional outcome (Schwartz and Moalem, 2001; Kim et al., 2014; Kim et al., 2012). The neutrophil-to-lymphocyte

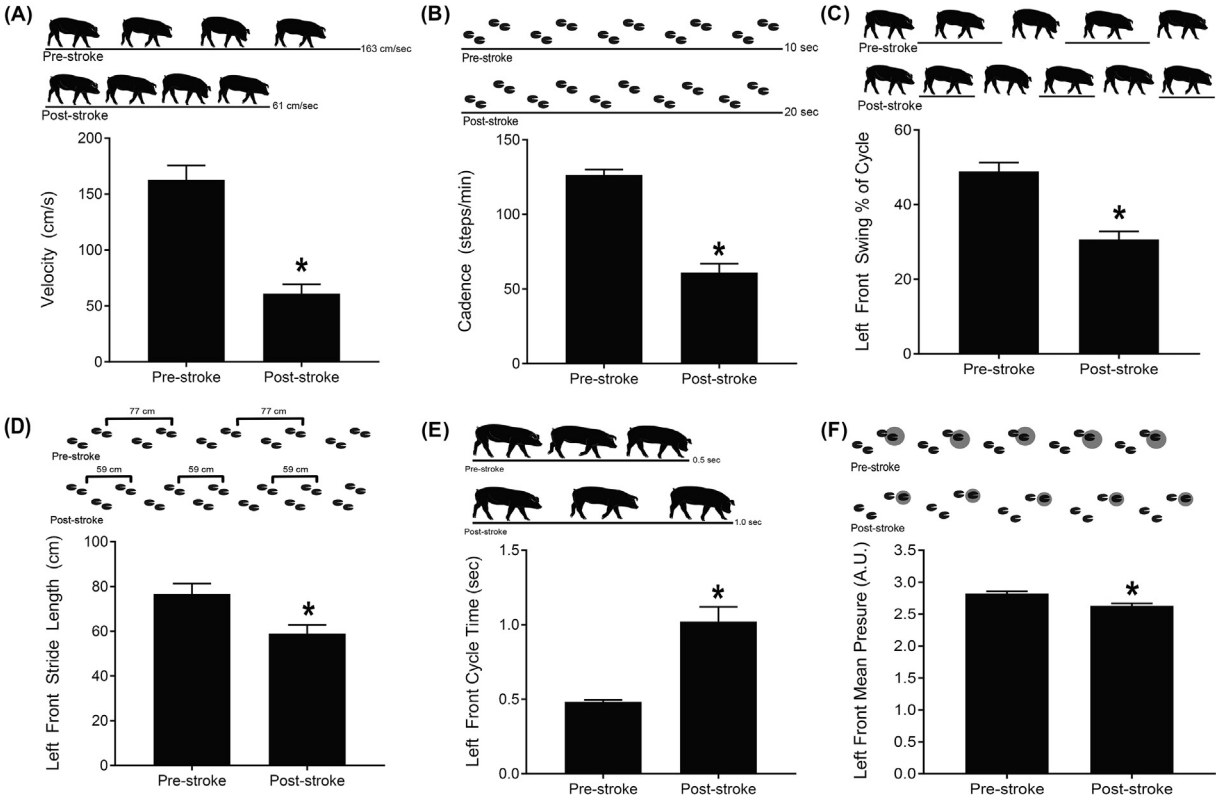

Fig. 6. Ischemic stroke resulted in spatiotemporal gait deficits. Velocity and cadence significantly ($p < 0.01$) decreased post-stroke (61.01 ± 8.39 vs. 162.9 ± 12.73 cm/s and 61.01 ± 5.91 vs. 126.44 ± 3.72 steps/min, respectively, A-B). The LF swing percent of cycle significantly ($p < 0.01$) decreased compared to pre-stroke (30.70 ± 2.12 vs. 48.89 ± 2.35%, respectively, C). A significant ($p < 0.01$) decrease in LF stride length was observed post-stroke compared to pre-stroke (59.04 ± 3.85 vs. 76.72 ± 4.60 cm, respectively, D). LF cycle time significantly ($p < 0.01$) increased relative to pre-stroke (1.02 ± 0.09 vs. 0.48 ± 0.013 sec, respectively, E). The mean pressure exhibited by the LF significantly ($p < 0.01$) decreased at post-stroke compared to pre-stroke (2.62 ± 0.03 vs. 2.82 ± 0.03 arbitrary units (A.U.), respectively, F). * indicates significant difference between pre-stroke and post-stroke time points.

ratio (NLR) was determined to be a useful marker to predict neurological deterioration and short-term mortality in patients with acute ischemic stroke (Xue et al., 2017; Zhang et al., 2017). Elevated NLRs have been reported to be associated with chronic inflammation, poor functional prognosis, and larger lesion volumes in ischemic stroke patients (Pikija et al., 2018; Suh et al., 2017; Lattanzi et al., 2017). These results suggest that neutrophil recruitment in our pig model may play a significant role in inflammatory-mediated secondary injury processes that contribute to the development of functional impairments. Furthermore, like stroke patients, neutrophil and lymphocyte levels in our pig model may also serve as ideal markers for stroke severity and outcome prediction.

OF testing is regularly used to evaluate neurobehavioral changes in response to experimental stroke (Balkaya et al., 2013; Crawley, 1985). As inherently inquisitive animals, pigs frequently demonstrate sniffing behavior during environmental and OF exploration (Studnitz and Margit Bak; Pedersen, Lene Juul. , 2007; Meunier-Salaun et al., 1991; Zebunke et al., 2013). In response to stroke however, significant reductions in exploratory perimeter sniffing was noted in our pigs and closely mirrored decreased exploratory behaviors observed in rodents post-stroke (Zhang et al., 2016; Wang et al., 2009). This lack of exploratory behavior in rodents has been attributed to anhedonia and early signs of depression in piglets (Wang et al., 2009; Kanitz et al., 2004; Cojocaru et al., 2013). Similarly, neurobehavioral changes including depression and apathy have been reported and correlated with inhibited recovery in stroke patients (Chemerinski and Robinson, 2000). Changes in pigs' spontaneous locomotion were marginal with no significant reductions in OF distance traveled or velocity observed. Although these observations contradict previously discussed results (gait velocity) it is likely due to fundamental differences between OF testing and gait analysis paradigms. During OF testing, pigs were permitted to ambulate at a self-selected speed (walk), whereas during gait collection pigs were preconditioned to ambulate at a consistent, 2-beat pace (jog) and received positive reinforcement for each successful gait performance. Gait collection maintained at a specific pace ensured consistency between all pigs and across time points. This allowed for gait deteriorations to be attributed to stroke-induced motor function changes and not differences in gait selection (walking vs. jogging) between pigs. Furthermore, 2-beat paces (jog) in quadrupeds requires increased balance and coordination compared to 4-beat paces (walk), thus resulting in improved sensitivity to detect gait deficits post-stroke. Collectively, these measures hold value for future assessments of therapeutic functional efficacy in characterizing exploratory behavior and changes in self-selected motor function.

In this study, we replicated patient cellular, tissue, and functional-level outcomes in pig model of acute ischemic stroke. MCAO in our pig model exhibited a multifactorial effect, thus leading to cytotoxic edema, lesioning, hemispheric swelling, and ICH while also decreasing diffusivity and WM integrity. These structural changes correlated with behavior and motor deficits in a similar manner to acute stroke patients. Although the rete mirabile limited reperfusion assessment, this model still possesses significant value as it not only adheres to STAIR recommendations by primarily testing in a permanent MCAO model, but also represents approximately 73–77% of patients with large vessel occlusion that do not regain tissue perfusion via spontaneous reperfusion, tPA, or embolectomy (McBride and Zhang, 2017; Stroke Therapy Academic, 1999). As an effective model of acute ischemic stroke pathophysiology, the pig model is potentially an excellent tool for identifying potential treatment targets and testing novel therapeutics and diagnostics.

4. Materials and methods

4.1. Animals and housing

All work performed in this study was approved by the University of Georgia (UGA) Institutional Animal Care and Use Committee (IACUC; Protocol Number: 2017–07-019Y1A0) and in accordance with the National Institutes of Health Guide for the Care and Use of Laboratory Animals guidelines. Six, sexually mature, castrated male Landrace pigs [48–56 kg/5–6 months] were purchased from the UGA Swine Unit and enrolled in this study. Male pigs were used in accordance with the STAIR guidelines that suggests initial therapeutic evaluations should be performed with young, healthy male animals (Lapchak et al., 2013). Furthermore, the authors believe this age group of sexually mature pigs is relevant as stroke is the 5th leading cause of death in individuals 15–59 years old (WHO, 2004; Greenlund et al., 2004). Pigs were individually housed in a Public Health Service (PHS) and Association for Assessment and Accreditation of Laboratory Animal Care (AAALAC) approved facility at a room temperature approximately 27 °C with a 12 h light/dark cycle. Pigs were given access to water and fed standard UGA grower 1 diets (Supplemental Fig. 2) with provision of enrichment through daily human contact and toys.

4.2. Study design

The sample size for this study (n = 5) was determined by a power calculation based on our routine use of the MCAO model with lesion volume changes by MRI imaging being the primary endpoint. The power analysis was calculated using a two-tailed ANOVA test, $\alpha = 0.05$, and an 80% power of detection effect size of 1.19 and a standard deviation of 44.63.

A total of six animals were enrolled in this study with two pigs randomly assigned to 1 of 3 surgical days. All endpoints and functional measurements were prospectively planned and underwent blinded analysis. Predefined exclusion criteria from all endpoints included instances of infection at the incision site, self-inflicted injuries that required euthanasia, inability to thermoregulate, uncontrolled seizure activity, and/or respiratory distress. Pigs were euthanized via lethal intravenous (IV) injection of euthanasia solution (1 mL/4.5 kg; VetOne). One pig was excluded from MRI collection as well as post-stroke blood and functional analysis due cerebellar herniation and consequently, premature death. No outliers were removed from the data.

4.3. Middle cerebral artery occlusion surgical procedures

The day prior to surgery, pigs were administered antibiotics (Excede; 5 mg/kg intramuscular (IM); Zoetis) and fentanyl for pain management (fentanyl patch; 100 mg/kg/hr transdermal (TD); Mayne Pharma). Pre-induction analgesia and sedation were achieved using xylazine (2 mg/kg IM; VetOne) and midazolam (0.2 mg/kg IM; Heritage). Anesthesia was induced with IV propofol (Zoetis) to effect and prophylactic lidocaine (1.0 mL 2% lidocaine; VetOne) topically to the laryngeal folds to facilitate intubation. Anesthesia was maintained with isoflurane (1.0–2.0%; Abbott Laboratories) in oxygen and air with vitals including temperature, respiration, heart rate, and blood pressure continuously monitored and maintained within normal parameters.

As previously described, ischemic stroke was induced via MCAO (Platt et al., 2014). Briefly, a curvilinear skin incision extended from the right orbit to an area rostral to the auricle. A segment of zygomatic arch was resected while the temporal fascia and muscle were elevated and a craniectomy was performed utilizing craniotome air drill (3 M C100). After exposing the local dura mater, the distal MCA and associated branches were permanently occluded using bipolar cautery forceps. The exposed brain was then covered with sterile biograft made of porcine small intestine submucosa (MatriStem, ACell). The temporalis muscle and epidermis were routinely re-apposed.

Anesthesia was discontinued and pigs were returned to their pens upon extubation and monitored every 15 min until vitals including temperature, heart rate, and respiratory rate returned to normal, every 4 h for 24 h, and twice a day thereafter until post-MCAO sutures were removed. Banamine (2.2 mg/kg IM; Merck) was administered for pain relief, acute inflammation, and fever management every 12 h for the first 24 h, and every 24 h for 3 days post-stroke.

4.4. Magnetic resonance imaging acquisition and analysis

MRI was performed pre- and 24 h post-stroke on a General Electric 3.0 Tesla MRI system. Pigs were sedated and maintained under anesthesia as previously described for MCAO surgery. MRI of the cranium was performed using an 8-channel torso coil with the pig positioned in supine recumbency. Multiplanar MRI sequences were acquired including T2FLAIR, T2W, T2*, DWI, and diffusion tensor imaging (DTI). Sequences were analyzed using Osirix software (Version 10.0.5) at default thresholds. Cytotoxic edema consistent with ischemic stroke was confirmed 24 h post-stroke by comparing corresponding hyperintense regions in T2FLAIR and DWI sequences and hypointense regions in ADC maps.

DWI sequences were collected utilizing b = 0 and b = 1000 and angles = L-R:0°; S-I:-21°. DWI lesions were identified by default thresholds of hyperintensity in each axial slice and the area of each lesion was multiplied by the slice thickness (2 mm) to obtain the total lesion volume. DWI sequences were collected in opposite phase directions (DWI-4 nex and DWI-4 nex pepolar) to further correct for potential distortions. Corresponding ADC regions of interest (ROI) were identified by default thresholds of hypointensity for each axial slice. An identical ROI was directly copied to the contralateral hemisphere for each axial slice. Mean ADC values of the ipsilateral and contralateral hemispheres were obtained by calculating the average signal intensity across all slices and reported as 10^{-3} mm^2/s. Hemisphere volumes were calculated using T2W sequences for each axial slice by manually outlining the ipsilateral and contralateral hemispheres. The hemisphere areas were multiplied by the slice thickness (3 mm) to obtain total hemisphere volumes. ICH volumes were calculated by manually outlining areas of hypointensity on T2* sequences and the hemorrhage areas were multiplied by the slice thickness (3 mm) to obtain total hemorrhage volumes. MLS was calculated utilizing T2W sequences for each axial slice by measuring the distance from the natural midline along the anterior and posterior attachments of the falx cerebri to the septum pellucidum. DTI was utilized to generate FA maps. FA values of the ICs were calculated manually on one representative slice per pig and were expressed as a percent change in the ipsilateral hemisphere relative to the contralateral hemisphere.

4.5. Blood collection and analysis

500 μL blood samples were collected from ear veins following topical application of 2.5% lidocaine and 2.5% prilocaine cream (Actavis) pre-stroke, 4, 12, and 24 h post-stroke into K2EDTA spray coated tubes (Patterson Veterinary). 4 μL of blood was pipetted onto the base of a ColorFrost microscope slide (ThermoScientific) approximately 1 cm from the edge. At an angle of approximately 45°, a spreader slide was placed in front of the blood and retracted until the blood sample evenly spread along the width of the slide. Even pressure on the spreader slide was applied in a forward direction in order to create a smear. Care was taken to ensure each blood smear covered two-thirds of the slide and exhibited an oval feathered end. Each slide was air dried [10 min], fixed with methanol [2 min], air dried [2 min], and then stained in Wright-Giemsa stain [5 min]. The stained slide was submerged in distilled water (dH_2O) [10 min]. Finally, the slide was rinsed, air dried, and then a cover slip was applied using Phosphate Buffered Saline (PBS). A trained, blinded researcher completed manual lymphocyte,

neutrophil, and band cells counts to maintain consistency between pigs across all time points. The first 100 white blood cells visualized at the monolayer, beginning approximately 1 mm away from the body of the smear, were recorded and expressed as a percentage.

4.6. Gait analysis

Pigs underwent gait analysis pre-stroke and 48 h post-stroke to assess changes in spatiotemporal gait parameters. Data was recorded using a GAITFour® electronic, pressure-sensitive mat (CIR Systems Inc.) 7.01 m in length and 0.85 m in width with an active area that is 6.10 m in length and 0.61 m in width. In this arrangement, the active area is a grid, 48 sensors wide by 480 sensors long, totaling 23,040 sensors. 2 weeks pre-stroke, pigs were trained to travel across a gait mat at a consistent, 2-beat pace. To reinforce consistency, rewards were given at each end of the mat for successful runs. Pre-stroke gait data was collected on 3 separate days for each pig. At each time point, pigs were encouraged to move along the mat until 5 consistent trials were collected with no more than 15 total trials accrued. As quadrupeds, pigs inherently distribute approximately 60% of their body weight to the forelimbs and40% to the hindlimbs.

Gait data was semi-automatically analyzed using GAITFour® Software (Version 4.9X9i) to provide quantitative measurements of velocity (cm/sec) and cadence (steps/min). Additional measurements were quantified specifically for the hemiparetic LF as the limbs contralateral to the stroke lesion typically exhibit more pronounced motor deficits relative to the ipsilateral limbs in humans, mice, and rats and the forelimbs in quadrupeds carry approximately 60% of the body weight (Hetze et al., 2012; Vandeputte et al., 2010). Consequently, the LF is the most affected post-stroke. These measurements included stride length (the distance between successive ground contact of the same hoof), swing percent of cycle (the percent of a full gait cycle in which a limb is not in contact with the ground), cycle time (the amount of time for a full stride cycle), swing time (the amount of time a limb is in the swing phase, or not in contact with the ground), and mean pressure (the amount of pressure exerted by a limb).

4.7. Open field testing

As an additional measure of functional outcome, pigs underwent OF behavior testing pre-stroke and 48 h post-stroke. All tests took place in a 2.7 m × 2.7 m arena lined with black rubber matting, used to provide stable footing. White curtains were hung around the arena to reduce visual distractions during testing. Trials [10 min] were recorded using EthoVision video tracking software (Version 11.5; Noldus Systems) to obtain objective and quantifiable measures of behavioral characteristics including velocity, distance traveled, and exploration. Specifically, perimeter wall sniffing (red lines), an exploratory behavior typical of pigs, was manually tracked and coded in the EthoVision software by trained personnel.

4.8. Statistical analysis

All quantitative data was analyzed with GraphPad Prism (Version 8) and statistical analysis software (SAS; Version 9.3). For MRI, behavior, and gait analyses, statistical significance was determined by a paired *t*-test. For white blood cell analysis, statistical significance was determined using proc mixed for repeated measures over time with time as the fixed effect. A type AR statement was used to account for autoregressive covariance. White blood cell counts at individual time points were compared with a post hoc PDIFF comparison. Comparisons where p-values ≤ 0.05 were considered significantly different. Data is reported as mean ± standard errors of the mean.

Declaration of Competing Interest

The authors declare that they have no known competing financial interests or personal relationships that could have appeared to influence the work reported in this paper.

Acknowledgements

The authors would like to thank Brandy Winkler and our team of undergraduate researchers who were involved in various aspects of surgeries, post-operative care, pig gait/behavioral testing, and data analysis. We would also like to thank the UGA Animal Resources team for veterinary care and guidance as well as Rick Utley and Kelly Parham for their pig expertise and management skills. We would like to thank Samantha Spellicy for her assistance with MLS and blood analysis.

Funding

This work was supported by the National Institute of Neurological Disorders and Stroke [grant number R01NS093314].

Appendix A. Supplementary data

Supplementary data to this article can be found online at https://doi.org/10.1016/j.brainres.2020.146778.

References

WHO, 2004. publishes definitive atlas on global heart disease and stroke epidemic. Indian J. Med. Sci. 58 (9), 405–406.
Savitz, S.I., Chopp, M., Deans, R., Carmichael, T., Phinney, D., Wechsler, L., et al., 2011. Stem Cell Therapy as an Emerging Paradigm for Stroke (STEPS) II. Stroke 42 (3), 825–829.
Fisher, M., Feuerstein, G., Howells, D.W., Hurn, P.D., Kent, T.A., Savitz, S.I., et al., 2009. Update of the stroke therapy academic industry roundtable preclinical recommendations. Stroke 40 (6), 2244–2250.
Kaiser, E.E., West, F.D., 2019. Large animal ischemic stroke models: replicating human stroke pathophysiology. Neural. Regen. Res.
Platt, S.R., Holmes, S.P., Howerth, E.W., Duberstein, K.J., Dove, C.R., Kinder, H.A., et al., 2014. Development and characterization of a Yucatan miniature biomedical pig permanent middle cerebral artery occlusion stroke model. Exp. Transl. Stroke. Med. 6 (1), 5.
Baker, E.W., Platt, S.R., Lau, V.W., Grace, H.E., Holmes, S.P., Wang, L., et al., 2017. Induced Pluripotent Stem Cell-Derived Neural Stem Cell Therapy Enhances Recovery in an Ischemic Stroke Pig Model. Sci. Rep. 7 (1), 10075.
Webb, R.L., Kaiser, E.E., Jurgielewicz, B.J., Spellicy, S., Scoville, S.L., Thompson, T.A., et al., 2018. Human Neural Stem Cell Extracellular Vesicles Improve Recovery in a Porcine Model of Ischemic Stroke. Stroke 49 (5), 1248–1256.
Vilela, P., Rowley, H.A., 2017. Brain ischemia: CT and MRI techniques in acute ischemic stroke. Eur. J. Radiol. 96, 162–172.
Rudkin, S., Cerejo, R., Tayal, A., Goldberg, M.F., 2018. Imaging of acute ischemic stroke. Emerg. Radiol. 25 (6), 659–672.
Tong, D.C., Yenari, M.A., Albers, G.W., O'Brien, M., Marks, M.P., Moseley, M.E., 1998. Correlation of perfusion- and diffusion-weighted MRI with NIHSS score in acute (< 6.5 hour) ischemic stroke. Neurology. 50 (4), 864–870.
Barber, P.A., Darby, D.G., Desmond, P.M., Yang, Q., Gerraty, R.P., Jolley, D., et al., 1998. Prediction of stroke outcome with echoplanar perfusion- and diffusion-weighted MRI. Neurology. 51 (2), 418–426.
Attye, A., Boncoeur-Martel, M.P., Maubon, A., Mounayer, C., Couratier, P., Labrunie, A., et al., 2012. Diffusion-Weighted Imaging infarct volume and neurologic outcomes after ischemic stroke. J. Neuroradiol. 39 (2), 97–103.
Warach, S., Gaa, J., Siewert, B., Wielopolski, P., Edelman, R.R., 1995. Acute human stroke studied by whole brain echo planar diffusion-weighted magnetic resonance imaging. Ann. Neurol. 37 (2), 231–241.
Lutsep, H.L., Albers, G.W., DeCrespigny, A., Kamat, G.N., Marks, M.P., Moseley, M.E., 1997. Clinical utility of diffusion-weighted magnetic resonance imaging in the assessment of ischemic stroke. Ann. Neurol. 41 (5), 574–580.
Lovblad, K.O., Laubach, H.J., Baird, A.E., Curtin, F., Schlaug, G., Edelman, R.R., et al., 1998. Clinical experience with diffusion-weighted MR in patients with acute stroke. AJNR Am. J. Neuroradiol. 19 (6), 1061–1066.
Baltan, S., Besancon, E.F., Mbow, B., Ye, Z., Hamner, M.A., Ransom, B.R., 2008. White matter vulnerability to ischemic injury increases with age because of enhanced excitotoxicity. J. Neurosci. 28 (6), 1479–1489.
Nakamura, M., Imai, H., Konno, K., Kubota, C., Seki, K., Puentes, S., et al., 2009. Experimental investigation of encephalomyosynangiosis using gyrencephalic brain of the miniature pig: histopathological evaluation of dynamic reconstruction of vessels for functional anastomosis. Laboratory investigation. J Neurosurg Pediatr. 3 (6),

488–495.
Liu, G., Dang, C., Chen, X., Xing, S., Dani, K., Xie, C., et al., 2015. Structural remodeling of white matter in the contralesional hemisphere is correlated with early motor recovery in patients with subcortical infarction. Restor. Neurol. Neurosci. 33 (3), 309–319.
Wang, Y., Liu, G., Hong, D., Chen, F., Ji, X., Cao, G., 2016. White matter injury in ischemic stroke. Prog. Neurobiol. 141, 45–60.
Li, M., Tian, S., Sun, L., Chen, X., 2019. Gait Analysis for Post-Stroke Hemiparetic Patient by Multi-Features Fusion Method. Sensors (Basel) 19 (7).
Boudarham, J., Roche, N., Pradon, D., Bonnyaud, C., Bensmail, D., Zory, R., 2013. Variations in kinematics during clinical gait analysis in stroke patients. PLoS ONE 8 (6), e66421.
Nascimento, L.R., de Oliveira, C.Q., Ada, L., Michaelsen, S.M., Teixeira-Salmela, L.F., 2015. Walking training with cueing of cadence improves walking speed and stride length after stroke more than walking training alone: a systematic review. J. Physiother. 61 (1), 10–15.
Hak, L., Houdijk, H., van der Wurff, P., Prins, M.R., Beek, P.J., van Dieen, J.H., 2015. Stride frequency and length adjustment in post-stroke individuals: influence on the margins of stability. J. Rehabil. Med. 47 (2), 126–132.
Peterson, C.L., Hall, A.L., Kautz, S.A., Neptune, R.R., 2010. Pre-swing deficits in forward propulsion, swing initiation and power generation by individual muscles during hemiparetic walking. J. Biomech. 43 (12), 2348–2355.
Nolan, K.J., Yarossi, M., McLaughlin, P., 2015. Changes in center of pressure displacement with the use of a foot drop stimulator in individuals with stroke. Clin. Biomech. (Bristol, Avon). 30 (7), 755–761.
De Nunzio, A., Zucchella, C., Spicciato, F., Tortola, P., Vecchione, C., Pierelli, F., et al., 2014. Biofeedback rehabilitation of posture and weightbearing distribution in stroke: a center of foot pressure analysis. Funct. Neurol. 29 (2), 127–134.
Lind, N.M., Moustgaard, A., Jelsing, J., Vajta, G., Cumming, P., Hansen, A.K., 2007. The use of pigs in neuroscience: modeling brain disorders. Neurosci. Biobehav. Rev. 31 (5), 728–751.
Craner, S.L., Ray, R.H., 1991. Somatosensory cortex of the neonatal pig: I. Topographic organization of the primary somatosensory cortex (SI). J. Comp. Neurol. 306 (1), 24–38.
Michael, K.M., Allen, J.K., Macko, R.F., 2005. Reduced ambulatory activity after stroke: the role of balance, gait, and cardiovascular fitness. Arch. Phys. Med. Rehabil. 86 (8), 1552–1556.
Lovblad, K.O., Baird, A.E., Schlaug, G., Benfield, A., Siewert, B., Voetsch, B., et al., 1997. Ischemic lesion volumes in acute stroke by diffusion-weighted magnetic resonance imaging correlate with clinical outcome. Ann. Neurol. 42 (2), 164–170.
Schellinger, P.D., Jansen, O., Fiebach, J.B., Hacke, W., Sartor, K., 1999. A standardized MRI stroke protocol: comparison with CT in hyperacute intracerebral hemorrhage. Stroke 30 (4), 765–768.
Jokinen, H., Gouw, A.A., Madureira, S., Ylikoski, R., van Straaten, E.C., van der Flier, W.M., et al., 2011. Incident lacunes influence cognitive decline: the LADIS study. Neurology. 76 (22), 1872–1878.
Ahmad, A.S., Satriotomo, I., Fazal, J., Nadeau, S.E., Dore, S., 2015. Considerations for the Optimization of Induced White Matter Injury Preclinical Models. Front. Neurol. 6, 172.
Srikanth, V., Beare, R., Blizzard, L., Phan, T., Stapleton, J., Chen, J., et al., 2009. Cerebral white matter lesions, gait, and the risk of incident falls: a prospective population-based study. Stroke 40 (1), 175–180.
Pikija, S., Sztriha, L.K., Killer-Oberpfalzer, M., Weymayr, F., Hecker, C., Ramesmayer, C., et al., 2018. Neutrophil to lymphocyte ratio predicts intracranial hemorrhage after endovascular thrombectomy in acute ischemic stroke. J. Neuroinflammation. 15 (1), 319.
Guo, Z., Yu, S., Xiao, L., Chen, X., Ye, R., Zheng, P., et al., 2016. Dynamic change of neutrophil to lymphocyte ratio and hemorrhagic transformation after thrombolysis in stroke. J. Neuroinflammation. 13 (1), 199.
Song, Q., Li, Y., Wang, Y., Wei, C., Liu, J., Liu, M., 2018. Increased Neutrophil-to-lymphocyte Ratios are Associated with Greater Risk of Hemorrhagic Transformation in Patients with Acute Ischemic Stroke. Curr. Neurovasc. Res. 15 (4), 326–335.
Clark, P.C., Dunbar, S.B., Aycock, D.M., Courtney, E., Wolf, S.L., 2006. Caregiver perspectives of memory and behavior changes in stroke survivors. Rehabil Nurs. 31 (1), 26–32.
Alexander, L.D., Black, S.E., Patterson, K.K., Gao, F., Danells, C.J., McIlroy, W.E., 2009. Association between gait asymmetry and brain lesion location in stroke patients. Stroke 40 (2), 537–544.
Kumar, G., Goyal, M.K., Sahota, P.K., Jain, R., 2010. Penumbra, the basis of neuroimaging in acute stroke treatment: current evidence. J. Neurol. Sci. 288 (1–2), 13–24.
Saenger, A.K., Christenson, R.H., 2010. Stroke biomarkers: progress and challenges for diagnosis, prognosis, differentiation, and treatment. Clin. Chem. 56 (1), 21–33.
Yoo, A.J., Barak, E.R., Copen, W.A., Kamalian, S., Gharai, L.R., Pervez, M.A., et al., 2010. Combining acute diffusion-weighted imaging and mean transmit time lesion volumes with National Institutes of Health Stroke Scale Score improves the prediction of acute stroke outcome. Stroke 41 (8), 1728–1735.
Huisman, T.A., 2003. Diffusion-weighted imaging: basic concepts and application in cerebral stroke and head trauma. Eur. Radiol. 13 (10), 2283–2297.
Payabvash, S., Taleb, S., Benson, J.C., Rykken, J.B., Oswood, M.C., McKinney, A.M., et al., 2017. The Effects of DWI-Infarct Lesion Volume on DWI-FLAIR Mismatch: Is There a Need for Size Stratification? J. Neuroimaging 27 (4), 392–396.
Merino, J.G., Warach, S., 2010. Imaging of acute stroke. Nat. Rev. Neurol. 6 (10), 560–571.
Assemlal, H.E., Tschumperle, D., Brun, L., Siddiqi, K., 2011. Recent advances in diffusion MRI modeling: Angular and radial reconstruction. Med. Image Anal. 15 (4), 369–396.
Jha, S.K., 2003. Cerebral Edema and its Management. Med. J. Armed. Forces India. 59 (4), 326–331.
Liang, D., Bhatta, S., Gerzanich, V., Simard, J.M., 2007. Cytotoxic edema: mechanisms of pathological cell swelling. Neurosurg. Focus 22 (5), E2.
Berrouschot, J., Sterker, M., Bettin, S., Koster, J., Schneider, D., 1998. Mortality of space-occupying ('malignant') middle cerebral artery infarction under conservative intensive care. Intensive Care Med. 24 (6), 620–623.
Hacke, W., Schwab, S., Horn, M., Spranger, M., De Georgia, M., von Kummer, R., 1996. 'Malignant' middle cerebral artery territory infarction: clinical course and prognostic signs. Arch. Neurol. 53 (4), 309–315.
Arnaout, O.M., Aoun, S.G., Batjer, H.H., Bendok, B.R., 2011. Decompressive hemicraniectomy after malignant middle cerebral artery infarction: rationale and controversies. Neurosurg. Focus 30 (6), E18.
Vahedi, K., Hofmeijer, J., Juettler, E., Vicaut, E., George, B., Algra, A., et al., 2007. Early decompressive surgery in malignant infarction of the middle cerebral artery: a pooled analysis of three randomised controlled trials. Lancet Neurol. 6 (3), 215–222.
Wang, D.Z., Nair, D.S., Talkad, A.V., 2011. Acute Decompressive Hemicraniectomy to Control High Intracranial Pressure in Patients with Malignant MCA Ischemic Strokes. Curr Treat Options Cardiovasc Med. 13 (3), 225–232.
O'Collins, V.E., Macleod, M.R., Donnan, G.A., Horky, L.L., van der Worp, B.H., Howells, D.W., 2006. 1,026 experimental treatments in acute stroke. Ann. Neurol. 59 (3), 467–477.
Kotwica, Z., Hardemark, H.G., Persson, L., 1991. Intracranial pressure changes following middle cerebral artery occlusion in rats. Res Exp Med (Berl). 191 (2), 99–104.
Schirrmacher, R., Dea, M., Heiss, W.D., Kostikov, A., Funck, T., Quessy, S., et al., 2016. Which Aspects of Stroke Do Animal Models Capture? A Multitracer Micro-PET Study of Focal Ischemia with Endothelin-1. Cerebrovasc Dis. 41 (3–4), 139–147.
Hughes, P.M., Anthony, D.C., Ruddin, M., Botham, M.S., Rankine, E.L., Sablone, M., et al., 2003. Focal lesions in the rat central nervous system induced by endothelin-1. J. Neuropathol. Exp. Neurol. 62 (12), 1276–1286.
Fluri, F., Schuhmann, M.K., Kleinschnitz, C., 2015. Animal models of ischemic stroke and their application in clinical research. Drug Des Devel Ther. 9, 3445–3454.
Wells, A.J., Vink, R., Helps, S.C., Knox, S.J., Blumbergs, P.C., Turner, R.J., 2015. Elevated Intracranial Pressure and Cerebral Edema following Permanent MCA Occlusion in an Ovine Model. PLoS One 10 (6), e0130512.
Ropper, A.H., 1986. Lateral displacement of the brain and level of consciousness in patients with an acute hemispheral mass. N. Engl. J. Med. 314 (15), 953–958.
Treadwell, S.D., Thanvi, B., 2010. Malignant middle cerebral artery (MCA) infarction: pathophysiology, diagnosis and management. Postgrad. Med. J. 86 (1014), 235–242.
Walberer, M., Blaes, F., Stolz, E., Muller, C., Schoenburg, M., Tschernatsch, M., et al., 2007. Midline-shift corresponds to the amount of brain edema early after hemispheric stroke–an MRI study in rats. J. Neurosurg. Anesthesiol. 19 (2), 105–110.
Alharbi, B.M., Tso, M.K., Macdonald, R.L., 2016. Animal models of spontaneous intracerebral hemorrhage. Neurol. Res. 38 (5), 448–455.
Jaillard, A., Cornu, C., Durieux, A., Moulin, T., Boutitie, F., Lees, K.R., et al., 1999. Hemorrhagic transformation in acute ischemic stroke. The MAST-E study. MAST-E Group. Stroke. 30 (7), 1326–1332.
D'Amelio, M., Terruso, V., Famoso, G., Di Benedetto, N., Realmuto, S., Valentino, F., et al., 2014. Early and late mortality of spontaneous hemorrhagic transformation of ischemic stroke. J. Stroke Cerebrovasc. Dis. 23 (4), 649–654.
Fiorelli, M., Bastianello, S., von Kummer, R., del Zoppo, G.J., Larrue, V., Lesaffre, E., et al., 1999. Hemorrhagic transformation within 36 hours of a cerebral infarct: relationships with early clinical deterioration and 3-month outcome in the European Cooperative Acute Stroke Study I (ECASS I) cohort. Stroke 30 (11), 2280–2284.
Caceres, J.A., Goldstein, J.N., 2012. Intracranial hemorrhage. Emerg. Med. Clin. North Am. 30 (3), 771–794.
Sahni, R., Weinberger, J., 2007. Management of intracerebral hemorrhage. Vasc Health Risk Manag. 3 (5), 701–709.
Castro, P., Azevedo, E., Serrador, J., Rocha, I., Sorond, F., 2017. Hemorrhagic transformation and cerebral edema in acute ischemic stroke: Link to cerebral autoregulation. J. Neurol. Sci. 372, 256–261.
Zhang, J., Yang, Y., Sun, H., Xing, Y., 2014. Hemorrhagic transformation after cerebral infarction: current concepts and challenges. Ann. Transl. Med. 2 (8), 81.
Yaghi, S., Willey, J.Z., Cucchiara, B., Goldstein, J.N., Gonzales, N.R., Khatri, P., et al., 2017. Treatment and Outcome of Hemorrhagic Transformation After Intravenous Alteplase in Acute Ischemic Stroke: A Scientific Statement for Healthcare Professionals From the American Heart Association/American Stroke Association. Stroke 48 (12), e343–e361.
Biesbroek, J.M., Weaver, N.A., Biessels, G.J., 2017. Lesion location and cognitive impact of cerebral small vessel disease. Clin Sci (Lond). 131 (8), 715–728.
Lee, K.B., Kim, J.S., Hong, B.Y., Sul, B., Song, S., Sung, W.J., et al., 2017. Brain lesions affecting gait recovery in stroke patients. Brain. Behav. 7 (11), e00868.
Roth, E.J., Merbitz, C., Mroczek, K., Dugan, S.A., Suh, W.W., 1997. Hemiplegic gait. Relationships between walking speed and other temporal parameters. Am. J. Phys. Med. Rehabil. 76 (2), 128–133.
Titianova, E.B., Tarkka, I.M., 1995. Asymmetry in walking performance and postural sway in patients with chronic unilateral cerebral infarction. J. Rehabil. Res. Dev. 32 (3), 236–244.
Hidler, J.M., Carroll, M., Federovich, E.H., 2007. Strength and coordination in the paretic leg of individuals following acute stroke. IEEE Trans. Neural Syst. Rehabil. Eng. 15 (4), 526–534.
Duberstein, K.J., Platt, S.R., Holmes, S.P., Dove, C.R., Howerth, E.W., Kent, M., et al., 2014. Gait analysis in a pre- and post-ischemic stroke biomedical pig model. Physiol. Behav. 125, 8–16.
Chamorro, A., Hallenbeck, J., 2006. The harms and benefits of inflammatory and immune responses in vascular disease. Stroke 37 (2), 291–293.
Kleinig, T.J., Vink, R., 2009. Suppression of inflammation in ischemic and hemorrhagic stroke: therapeutic options. Curr. Opin. Neurol. 22 (3), 294–301.

Haeusler, K.G., Schmidt, W.U., Fohring, F., Meisel, C., Helms, T., Jungehulsing, G.J., et al., 2008. Cellular immunodepression preceding infectious complications after acute ischemic stroke in humans. Cerebrovasc Dis. 25 (1–2), 50–58.
Vogelgesang, A., Grunwald, U., Langner, S., Jack, R., Broker, B.M., Kessler, C., et al., 2008. Analysis of lymphocyte subsets in patients with stroke and their influence on infection after stroke. Stroke; A J. Cerebral Circulation 39 (1), 237–241.
Schwartz, M., Moalem, G., 2001. Beneficial immune activity after CNS injury: prospects for vaccination. J. Neuroimmunol. 113 (2), 185–192.
Kim, J.Y., Kawabori, M., Yenari, M.A., 2014. Innate inflammatory responses in stroke: mechanisms and potential therapeutic targets. Curr. Med. Chem. 21 (18), 2076–2097.
Kim, J., Song, T.J., Park, J.H., Lee, H.S., Nam, C.M., Nam, H.S., et al., 2012. Different prognostic value of white blood cell subtypes in patients with acute cerebral infarction. Atherosclerosis. 222 (2), 464–467.
Xue, J., Huang, W., Chen, X., Li, Q., Cai, Z., Yu, T., et al., 2017. Neutrophil-to-Lymphocyte Ratio Is a Prognostic Marker in Acute Ischemic Stroke. J. Stroke and Cerebrovascular Diseases: The Official J. National Stroke Assoc. 26 (3), 650–657.
Zhang, J., Ren, Q., Song, Y., He, M., Zeng, Y., Liu, Z., et al., 2017. Prognostic role of neutrophil-lymphocyte ratio in patients with acute ischemic stroke. Medicine (Baltimore). 96 (45), e8624.
Suh, B., Shin, D.W., Kwon, H.M., Yun, J.M., Yang, H.K., Ahn, E., et al., 2017. Elevated neutrophil to lymphocyte ratio and ischemic stroke risk in generally healthy adults. PLoS ONE 12 (8), e0183706.
Lattanzi, S., Cagnetti, C., Provinciali, L., Silvestrini, M., 2017. Neutrophil-to-lymphocyte ratio and neurological deterioration following acute cerebral hemorrhage. Oncotarget. 8 (34), 57489–57494.
Balkaya, M., Krober, J.M., Rex, A., Endres, M., 2013. Assessing post-stroke behavior in mouse models of focal ischemia. J. Cereb. Blood Flow Metab. 33 (3), 330–338.
Crawley, J.N., 1985. Exploratory behavior models of anxiety in mice. Neurosci. Biobehav. Rev. 9 (1), 37–44.
Studnitz, M.J., Bak, Margit, Pedersen, Lene Juul, 2007. Why do pigs root and in what will they root?: A review on the exploratory behaviour of pigs in relation to environmental enrichment. Appl. Animal Behav. Sci. 107 (3–4), 183–197.
Meunier-Salaun, M.C., Monnier, M., Colleaux, Y., Seve, B., Henry, Y., 1991. Impact of dietary tryptophan and behavioral type on behavior, plasma cortisol, and brain metabolites of young pigs. J. Anim. Sci. 69 (9), 3689–3698.
Zebunke, M., Puppe, B., Langbein, J., 2013. Effects of cognitive enrichment on behavioural and physiological reactions of pigs. Physiol. Behav. 118, 70–79.
Zhang, C., Meng, Q., Zhang, X., Wu, S., Wang, S., Chen, R., et al., 2016. Role of astrocyte activation in fine particulate matter-enhancement of existing ischemic stroke in Sprague-Dawley male rats. J. Toxicol. Environ. Health A. 79 (9–10), 393–401.
Wang, S.H., Zhang, Z.J., Guo, Y.J., Zhou, H., Teng, G.J., Chen, B.A., 2009. Anhedonia and activity deficits in rats: impact of post-stroke depression. J. Psychopharmacol. 23 (3), 295–304.
Kanitz, E., Tuchscherer, M., Puppe, B., Tuchscherer, A., Stabenow, B., 2004. Consequences of repeated early isolation in domestic piglets (Sus scrofa) on their behavioural, neuroendocrine, and immunological responses. Brain Behav. Immun. 18 (1), 35–45.
Cojocaru, G.R., Popa-Wagner, A., Stanciulescu, E.C., Babadan, L., Buga, A.M., 2013. Post-stroke depression and the aging brain. J. Mol. Psychiatry 1 (1), 14.
Chemerinski, E., Robinson, R.G., 2000. The neuropsychiatry of stroke. Psychosomatics. 41 (1), 5–14.
McBride, D.W., Zhang, J.H., 2017. Precision Stroke Animal Models: the Permanent MCAO Model Should Be the Primary Model. Not Transient MCAO, Transl Stroke Res.
Stroke Therapy Academic, 1999. Industry R. Recommendations for standards regarding preclinical neuroprotective and restorative drug development. Stroke 30 (12), 2752–2758.
Lapchak, P.A., Zhang, J.H., Noble-Haeusslein, L.J., 2013. RIGOR guidelines: escalating STAIR and STEPS for effective translational research. Translational stroke research. 4 (3), 279–285.
Greenlund, K.J., Croft, J.B., Mensah, G.A., 2004. Prevalence of heart disease and stroke risk factors in persons with prehypertension in the United States, 1999–2000. Arch. Intern. Med. 164 (19), 2113–2118.
Hetze, S., Romer, C., Teufelhart, C., Meisel, A., Engel, O., 2012. Gait analysis as a method for assessing neurological outcome in a mouse model of stroke. J. Neurosci. Methods 206 (1), 7–14.
Vandeputte, C., Taymans, J.M., Casteels, C., Coun, F., Ni, Y., Van Laere, K., et al., 2010. Automated quantitative gait analysis in animal models of movement disorders. BMC Neurosci. 11, 92.